

## **ROSIGLITAZONE NANOPARTICLES LOADED IN HYDROGEL FOR THE ACCELERATED HEALING OF FULL THICKNESS EXCISION WOUNDS IN DIABETIC RATS**

**Mohammed Tajuddin<sup>1</sup>, Rakesh Kumar Jat<sup>2</sup> and Nagakanyaka Devi Paladugu<sup>3\*</sup>**

<sup>1</sup>Department of Pharmacology, Shri Jagdishprasad Jhabarmal Tibrewala University, Jhunjhunu, Rajasthan, India.

<sup>2</sup>Department of Pharmaceutical Chemistry, Shri Jagdishprasad Jhabarmal Tibrewala University, Jhunjhunu, Rajasthan, India.

<sup>3</sup>Department Pharmaceutics, Max Institute of Pharmaceutical Sciences, Khammam, Telangana, India.

Article Received on  
21 June 2020,

Revised on 11 July 2020,  
Accepted on 01 August 2020,

DOI: 10.20959/wjpr20208-18344

### **\*Corresponding Author**

**Nagakanyaka Devi  
Paladugu**

Department Pharmaceutics,  
Max Institute of  
Pharmaceutical Sciences,  
Khammam, Telangana,  
India.

### **ABSTRACT**

Diabetic wound (DW) is a major problem which often requires amputation of the concerned organ in diabetic patients. In diabetes, the prolonged inflammation phase hinders the further phases of healing which, in turn, lead to improper healing of the wounds. Rosiglitazone (Ros) is an anti-diabetic drug with reported anti-inflammatory properties. The aim of the current study is to develop a Ros-chitosan nanoparticle (Ros-CS-NPs) loaded collagen hydrogel and evaluate its healing ability in DWs. The results of characterization of hydrogel reveal that the ROS-CS-NPs loaded hydrogel possess optimum particle size, controlled Ros release, biocompatibility and enhanced the cell migration. Using the streptozotocin and high fat induced DW model, significantly ( $p < 0.05$ ) faster rates of wound contraction in ROS-CS-

NPs loaded hydrogel treated group was observed in comparison with that in control and CS-NPs loaded hydrogel treated groups. The ELISA results indicate a significant ( $p < 0.05$ ) decrease of MMP-9 levels in the ROS-CS-NPs loaded hydrogel treated group as compared to those in control groups. Thus, the use of ROS-CS-NPs loaded hydrogel can prove to be a capable approach in the treatment of DWs.

**KEYWORDS:** Rosiglitazone; Chitosan nanoparticles; Collagen; Hydrogel and Diabetic wound.

## 1. INTRODUCTION

Diabetes mellitus (DM) is a metabolic disorder in which failure of the body to generate insulin or respond to it, leads to irregular metabolism of carbohydrates causing an increase of blood glucose.<sup>[1]</sup> Though the DM is treated in due course it causes several complications. Most frequent and devastating complication of DM is the diabetic wound (DW) which ends up with amputation of the concerned organ. As per the statistics by 'International diabetic federation' approximately 25% of diabetic patients are having a tendency to develop a DW in their life time.<sup>[2]</sup> The diminished healing of wound is attributed to other complication that were developed in due course of DM i.e. immunopathy, vasculopathy and neuropathy. If DW is left untreated, the wounds may turn into gangrene, far ahead leading to amputation.<sup>[3-5]</sup> Several treatment approaches such as patient education, monitoring blood sugar, wound debridement, pressure offloading, surgery and advanced therapies are in practice.<sup>[6, 7]</sup> None of the treatment approaches address all the necessary prerequisites of DW care because of the multifaceted pathophysiology and high cost related to these standard care treatments.<sup>[8, 9]</sup> Nonetheless, the pathogenesis of the DW is multifaceted, the prolonged inflammation along with inappropriate tissue management are reported to be the foremost reasons for diminished healing.<sup>[10,11]</sup>

The increased levels of inflammatory enzymes, particularly matrix metalloproteinases (MMPs) are stated to be the major cause for chronic inflammation.<sup>[12]</sup> In the family of MMPs, MMP-9 is the major metalloproteinase responsible for the degradation of formed matrix leading to improper matrix formation causing delayed healing.<sup>[13]</sup> Literature also suggests that the increased levels of MMP-9 was observed in chronic wound fluids compared to those of MMP-1, 2 and 8.<sup>[14]</sup> Inhibition of increased levels of MMP-9 is reported to accelerate the healing of wounds in DM condition.<sup>[14,15]</sup> Thus, local treatment with anti-inflammatory compounds that block the MMP-9, can reestablish the cutaneous homeostasis, proper matrix formation and faster healing.

Rosiglitazone (Ros), an antidiabetic drug with reported MMP-9 inhibition activity was chosen to suppress the major upregulated inflammatory mediator (MMP-9) responsible for continued inflammatory phase in DM condition.<sup>[16-18]</sup> Due to low solubility of Ros, nanoparticles (NPs) was prepared. For the formation of hydrogel containing Ros-NPs, collagen (COL) was selected. The COL was selected based on its unique biological properties such as cellular interactions and found to be abundant in extracellular matrix. It also provides

the structural matrix, that is accountable for significant healing of DW<sup>(19)</sup>. COL hydrogel containing Ros-NPs are, consequently, fabricated with the aim to counteract the inflammation in DWs and to enhance cell proliferation, differentiation and formation of structural matrix.

## 2. MATERIALS AND METHODS

The study was conducted in the animal house, located in department of pharmacology after getting approval from Institutional Animal ethics committee of Care College of Pharmacy- Warangal, Telangana, The study period was two months (60days).

### 2.1. Reagents and cell line

- Rosiglitazone hydrochloride (Sigma chemicals Co. Ltd, Mumbai, India).
- Chitosan medium molecular weight (Sigma chemicals Co. Ltd, Mumbai, India,).
- Type-1 collagen from rat tail (Sigma chemicals Co. Ltd, Mumbai).
- Lecithin (Merck Millipore, Mumbai, India).
- Methyl chloride (Thermo Fisher Scientific, Mumbai, India).
- Acetone (Merck Millipore, Mumbai, India).
- Poloxamer 188 (Thermo Fisher Scientific, Mumbai, India).
- Mouse embryonic fibroblast cells (3T3-L1) (National Centre for Cell Sciences, Pune, India).

Twenty four adult albino rats of either sex weighing 100–200 g were used for this study. The animals were allowed to acclimatize in the research laboratory for 1 week before the commencement of the study. The animals had been maintained under standard conditions (room temperature 25°C±3, humidity 35–60%, and light and dark period 12/12 h). All animals were fed with food and water ad libitum. All the animal testing were done under the approval of Institutional Animal Ethical Committee of Care College of Pharmacy, Warangal, Telangana.

### 2.2. Preparation of Chitosan NPs (CS-NPs) and gelatin NPs (GA-NPs) containing Ros

Ros is a practically water insoluble compound having log P value of 2.56. CS-NPs and GA-NPs were formulated by emulsion solvent diffusion technique. Initially, o/w emulsion was prepared by dissolving Ros (1% w/w) and lecithin (1.2% w/w) in methylene chloride followed by acetone respectively (3:1 ratio 12% w/w) to form oil phase. The obtained oil phase was injected into an aqueous phase containing poloxamer 188 (0.8% w/w) in the presence of CS (0.5% w/w) or GA (0.5% w/w), with continuous stirring, Then the prepared emulsion was

homogenized at a high pressure of 1000 bar for 5 min. Methylene chlorides was removed from the obtained emulsion at room temperature under condensed pressure using a rotavapor. The attained dispersion was filtered to isolate microspheres or agglomerates using a 1.0 mm cellulose ester milliporepaper. To completely remove the acetone in the resultant filtrate comprising NPs was diluted with 50 mL of millipore water. Further, the dispersion was centrifuged at 40,000 rpm for 20 min and the collected supernatant was discarded. Finally, the sediment of NPs was resuspended in 20 mL of millipore water to remove the traces of acetone. Again, the dispersion was recentrifuged and the obtained supernatant was discarded and final volume of the nanosuspension was adjusted to 10 ml with millipore water.<sup>[20]</sup>

### 2.3. Evaluation of Ros loaded CS-NPs and GA-NPs

#### 2.3.1. Particle size and zeta potential determination

Zeta potential and particle size of the prepared NPs were measured with the help of a size analyser have a facility to analyse zeta potential also (Malvern Instruments, USA). In addition, polydispersity index (PDI) was also measured to find out the size distribution range.<sup>[5, 20]</sup>

#### 2.3.2. Entrapment efficiency

Entrapment efficiency (EE) of the Ros in NPs was measured by means of the centrifugation technique.<sup>[5,20]</sup> The formulated NPS was subjected to cold centrifugation (Remi Equipment's Ltd, Mumbai, India) at 4°C with an rpm of 15,000 for 15 min. The supernatant was collected, diluted suitably and absorbance was measured at 241 nm. Amount of Ros entrapment in NPS was calculated using the below formula.

$$\text{Entrapment efficiency} = \frac{\text{amount of entrapped drug}}{\text{total amount of drug}} \times 100$$

### 2.4. Preparation of COL hydrogel

COL solution (1% w/v) was prepared using deionized water at room temperature. To, this solution either Ros-CS-NPs or ROS-GA-NPs was added and placed it in refrigerator for 30 min at 4 °C. Then, the ice-cold gel mixture was pipette out and transferred into a sterile round shaped aluminum container. The gel was left at room temperature for 15 to 20 min to undergo polymerize. Later, the aluminum container was covered and kept in incubator at 37 °C for an extra 60 min to finish polymerization<sup>(21, 22)</sup>.

## 2.5. Characterization of hydrogel

### 2.5.1. Physical examination

Physical examination of prepared hydrogels was a dynamic examination as it is more related to the organoleptic properties such as colour, greasiness, grittiness, softness, phase separation and ease of application which have been assessed for the formulated hydrogel<sup>(23, 24)</sup>.

### 2.5.2. pH determination

The pH determination of the formulated hydrogel was carried out by dipping the pH electrode in the hydrogel and the instrumental readings were noted down using a digital pH meter (pH 510, EUTECH instruments).

### 2.5.3. Viscosity measurement

The viscosity of the formulated hydrogel was determined by means of Brookfield viscometer using the spindle no.7, at 25°C, with a speed of 10 rpm (DV II plus, Brookfield).<sup>[24]</sup>

### 2.5.4. *In vitro* release studies

The release of the Ros from the various formulated hydrogel was analyzed by passing through the semi permeable membrane which was soaked in phosphate buffer saline overnight at pH 7.4. The membrane was arranged with a diffusion area of 1.813 cm<sup>2</sup> in a Franz diffusion cell, 10 mL of phosphate buffer saline pH 7.4 was used to fill the receiver chamber which was continuously stirred at 300 rpm. Water bath was maintained at a temperature of 37±0.5°C to mimic the temperature of the skin. 1 g of hydrogel formulation was placed on the diffusion barrier in the donor compartment. 1 mL of the solution from the receiver compartment were withdrawn and substituted with the same quantity of fresh medium, at frequent time intervals (0.25, 0.5, 0.75, 1, 2, 4, 6, 8, 10 and 12 h). The samples collected were analyzed by using UV spectrophotometry.<sup>[25]</sup>

### 2.5.5. Release kinetics

The mode of the drug release was determined using data obtained from the *in vitro* release studies using various release kinetic models such as zero order, first order, Hixson Crowell, Peppas and Higuchi model to observe the mode of drug release.<sup>[24, 26]</sup>

## 2.6. *In vitro* biocompatibility studies

3T3L1 cells were used to examine the cell adhesion and proliferation on the hydrogels. MTT [(3-(4, 5 di methyl thiazole-2 yl) -2, 5-diphenyl tetra zolium bromide)] assay was used to

assess the biocompatibility of the prepared hydrogel. Hydrogel of standard dimensions (15 mm diameter) was placed in each well of 24 well plate containing 2 mL of Dulbecco's Modified Eagle's Medium (DMEM). To each plate, 3T3L1 cells at a density  $1 \times 10^5$  cells/mL were seeded on the hydrogel surface. Microplate reader (Infinite F50, TECAN, Switzerland) was used to measure the absorbance at a wavelength of 450 nm(5).

### 2.7. *In vitro* scratch assay

Scratch assay was performed using 3T3L1 cells which were grown in the DMEM by augmenting with 10% PBS. The cells were seeded in the tissue culture plates with a confluence of approximately 70-80% as a monolayer. A scratch was completed using a 1 mL pipette tip. The plates were treated with fresh medium containing the test sample and allowed to kept aside for 48 h to encourage the growth of the cells. After the completion of the study, the cells were thoroughly washed and fixed with 4% formaldehyde. For micro scopical examination, the crystal violet was used to stain the cells.<sup>[24, 27]</sup>

### 2.8. *In vitro* antibacterial property

The antibacterial efficacy of the hydrogels was tested against *Staphylococcus aureus* (*S. aureus*) and Escherichia coli (*E. coli*). First, the bacteria were sub-cultured in suitable media to confirm their purity. Aliquots containing *S. aureus* and *E. coli* were spread separately over the surface of the agar to allow inoculation. Further, 200  $\mu$ L of hydrogel was sited at the center origin of the plate and subsequently incubated at 37 °C for 120 h. The zone of inhibition was measured at 120 h.<sup>[28]</sup>

### 2.9. *In vivo* wound healing study

To assess wound healing, healthy male Wistar albino rats of 6-12 weeks of age weighing 180-200 g were used. The optimized laboratory conditions were used to house the animals with free access to the standard chow diet and water for 10 days to get acclimatizes. DM was induced by administering streptozotocin (40 mg/kg) prepared in citrate 0.1 M buffer of pH 4.5, intraperitoneally. Monitoring the levels of blood glucose (Glucometer; AccuChek, USA) was started 2 days after induction. Animals with  $\geq 300$  mg/dl of blood glucose were detached from the group and scrutinized for 7 more days. Only the animals that established constant augmented blood glucose levels were considered for the current study. The wounding was performed on the dorsal region of an area measuring  $2 \times 2$  cm<sup>2</sup> under anesthetic conditions (Ketamine 100 mg/kg and xylazine mg/kg). The wounds under the control group were dressed properly with sterile gauze while the remaining groups were enclosed with the

corresponding hydrogels during the extent of study. Finally, all the animals were housed individually after the recovery from anesthesia and observed meticulously. Further, animals were segregated into three groups. Wounds in Group 1 or control were roofed with sterile gauze, group 2 animals were treated with CS-NPs loaded hydrogel (hydrogel without Ros or placebo) and group 3 animals were treated with Ros-CS-NPs loaded hydrogel (test group).<sup>[29]</sup>  
<sup>30]</sup> Percentage wound contraction was calculated using the formula.

*% wound contraction*

$$= \frac{\text{wound area on day 0} - \text{wound area on a particular day}}{\text{wound area on day 0}} \times 100$$

### 2.10. Hydroxyproline estimation

The wound skin was expunged cautiously on the day 7, 14 and 21 to hydroxyproline content. All the skin samples were hydrolyzed for 20 min by autoclaving at 120°C and 450 µL of Chloramine-T was added with gentle mixing and kept for 25 min at room temperature to endure oxidation. 500 µl of Ehrlich's reagent (p-dimethyl amino benzaldehyde in perchloric acid/n-propanol) was added to the above mixture, followed by incubation for 20 min at 65°C. The reddish-purple color complex was formed and measured spectrophotometrically at 550 nm. The hydroxyproline content in the skin tissue was expressed as µg/mg.<sup>[29]</sup>

### 2.11. Histo pathological studies

The wound tissues which were isolated on the day 7, 14 and 21, are fixed in 10% formalin (10%) prepared in neutralized buffer solution. Microtome was used to cut into pieces of 6 µm thickness. After mounting the sections on a glass slide the staining was performed using hematoxylin and eosin (H&E). The images were picturized under 40x magnification using motic microscope.

### 2.12. ELISA test

MMP-9 estimation using ELISA kit (R & D systems) was performed by following the instructions provided by the developer of the kit. Isolated tissue samples were minced using homogenizer and the resultant mixture was subjected to centrifugation. The supernatant thus obtained was diluted 100-folds with assay buffer. The concentration of MMP-9 in the samples were predicted on day 21 for all the groups (control, CS-NPs and Ros-CS-NPs loaded hydrogel).<sup>[31]</sup>



### 2.13. Statistical analysis

The results obtained were designated as Mean  $\pm$  SD. One Way Analysis of Variance (ANOVA) was used to determine statistical significance followed by Dunnet's post hoc test. Statistical analysis was done using Graph pad prism v5.01 (San Diego, CA, USA). The recorded values possessing  $p < 0.05$  or lower were considered as significant.

## 3. RESULTS AND DISCUSSION

### 3.1. Characterization of Ros-CS-NPs and Ros-GA-NPs

The prepared Ros-CS-NPs and Ros-GA-NPs were evaluated for particle size and zeta potential. Particles were found to lie in the size range of  $246.9 \pm 14.93$  nm for Ros-CS-NPs, whereas Ros-GA-NPs has shown particle size range of  $184.5 \pm 14.22$  nm. Ros-CS-NPs have a zeta potential of  $32.7 \pm 6.22$  mV when compared with Ros-GA-NPs ( $17.6 \pm 7.73$  mV) (Table 1). Due to the poor water solubility of Ros, first converted into NPs and then incorporated into COL hydrogel. The particle size of the Ros-CS-NPs was slightly greater than that of Ros-GA-NPs with more positive zeta potential. The increased in particle size and zeta potential may be due to high entrapment of Ros in CS-NPs. High positive zeta potential helps in the better adhesion to the negatively charged cell membrane. (Table -1).

**Table 1: Characterization of Ros-CS-NPs and Ros-GA-NPs.**

Type of NPs	Mean particle size (nm) $\pm$ SD	Zeta potential (mV) $\pm$ SD	Yield (%) $\pm$ SD	Entrapment efficiency (%) $\pm$ SD
Ros-CS-NPs	$246.9 \pm 14.93$	$32.7 \pm 6.22$	$90.65 \pm 5.38$	$95.87 \pm 4.58$
Ros-GA-NPs	$184.5 \pm 14.22$	$17.6 \pm 7.73$	$82.57 \pm 6.75$	$89.51 \pm 3.43$

### 3.2. Characterization of the Ros-CS-NPs and Ros-GA-NPs loaded hydrogel

The results of physical examination are shown in the table 2. The prepared hydrogel was colorless, with a smooth texture, non-greasy and free from grittiness with no phase separation. The pH and viscosity of Ros-CS-NPs loaded hydrogel formulation was found to be  $6.9 \pm 0.94$  and  $5608 \pm 28$  respectively. Whereas, pH and viscosity of Ros-GA-NPs loaded hydrogel was found to be  $7.1 \pm 0.90$  and  $5479 \pm 23$  respectively (Table 2).

**Table 2: Characterization of Ros-CS-NPs and Ros-GA-NPs loaded hydrogel.**

Formulation	pH	Phase separation	Greasiness	Grittiness	Viscosity (cps)
Ros-CS-NPs loaded hydrogel	$6.9 \pm 0.94$	Nil	Non	Non	$5608 \pm 28$
Ros-GA-NPs loaded hydrogel	$7.1 \pm 0.90$	Nil	Non	Non	$5479 \pm 23$



### 3.3. *In vitro* drug release studies using semipermeable membrane

The release profile of Ros from Ros-CS-NPs loaded hydrogel and Ros-GA-NPs loaded hydrogel was obtained by placing the hydrogels on the semipermeable membrane in the Franz diffusion cell. Cumulative percentage Ros release from both the formulations over a period of 96 h, is shown in fig 1. It was detected that drug concentration progressively amplified in the receptor chamber with rise in time. Ros-GA-NPs loaded hydrogel formulations have shown maximum drug release ( $91.5 \pm 4.1$  at 96 h) when compared to Ros-CS-NPs loaded hydrogel which showed only  $66.7 \pm 3.2$  at 96 h time interval. The delayed release of Ros from the Ros-CS-NPs loaded hydrogel may be attributed to greater particle size. In addition, particle size also influences the release of drug. Smaller particles possess a larger surface area-to-volume ratio; consequently, most of the drug accompanying with small particles would be at or near the surface of the particle, which eventually leads to faster drug release.<sup>[32]</sup> This can increase in number of administrations for Ros-GA-NPs loaded hydrogel. Based on the above results, only Ros-CS-NPs loaded hydrogel was selected and evaluated for further studies.

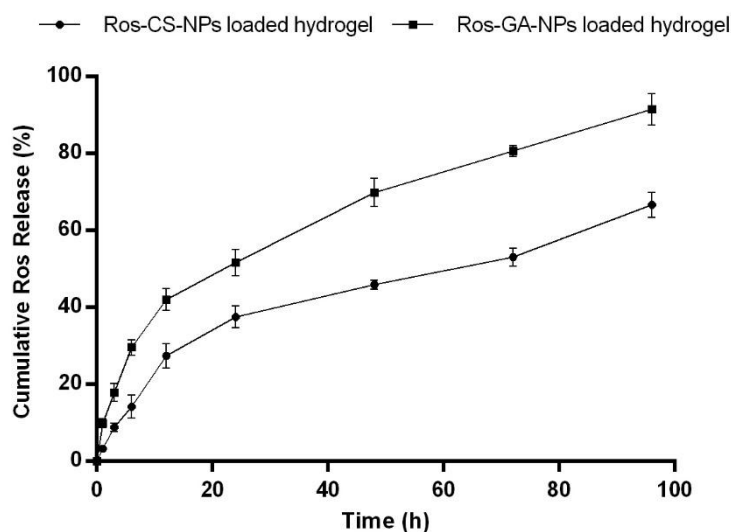


**Figure 1:** Cumulative percentage release of Ros from Ros-GA-NPs and Ros-CS-NPs loaded in hydrogel.

### 3.4. Release kinetics

The *in vitro* drug release data obtained from release study of Ros-CS-NPs loaded hydrogel were well fitted into numerous kinetic models like zero order, first order, Hixson Crowell, Higuchi and Korsmeyer-Peppas to analyze the mode of drug release. The values are accessible in table 3. The formulation was found to possess higher  $r^2$  value of 0.9827 for first

order kinetics which is near to 1.0, specifies the Ros is released at a persistent rate per unit time which is the goal line of all controlled release drug delivery systems.<sup>[33]</sup>

**Table 3: Release Kinetics of Ros-CS-NPs loaded hydrogel.**

	RELEASE KINETICS				
	ZERO	HIGUCHI	PEPPAS	FIRST	Hixson Crowell
	1	2	3	4	5
	R(CvT)	R(CvRoot(T))	Log T vs Log C	TIME vs LOG % REMAINING	TIME Vs (Q1/3-Qt1/3)
<b>Slope</b>	0.639	6.811	0.651	-0.007	0.014
<b>Correlation</b>	0.9467	0.9913	0.9818	-0.9778	0.9700
<b>R 2</b>	0.8962	0.9827	0.9639	0.9561	0.9409

### 3.5. *In vitro* biocompatibility and cell migration studies

The results clearly demonstrated that upon inclusion of the Ros-CS-NPs loaded hydrogel into the growth media did not stimulate any cytotoxicity of 3T3-L1 cells. The results of *in vitro* biocompatibility and cell migration studies are depicted in fig 2a and 2b. The results revealed that the prepared hydrogel was nontoxic and biocompatible. Moreover, cells treated with Ros-CS-NPs loaded hydrogel at concentration of 10-20 µg/mL exposed the significant augmented cell migration. The viability of cells and migration results further demonstrated that the hydrogels, regardless of the presence of Ros, were biocompatible with 3T3L1 cells.

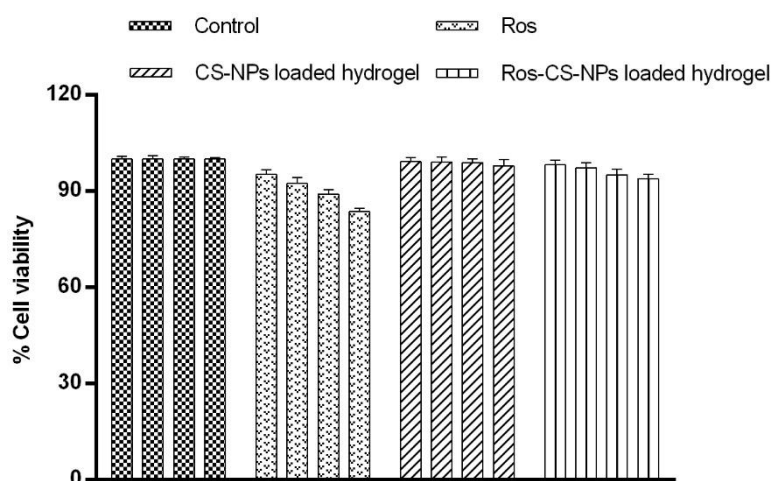


**Figure 2a: Cytotoxicity profile of Ros, CS-NPs loaded hydrogel and Ros-CS-NPs loaded hydrogel.**

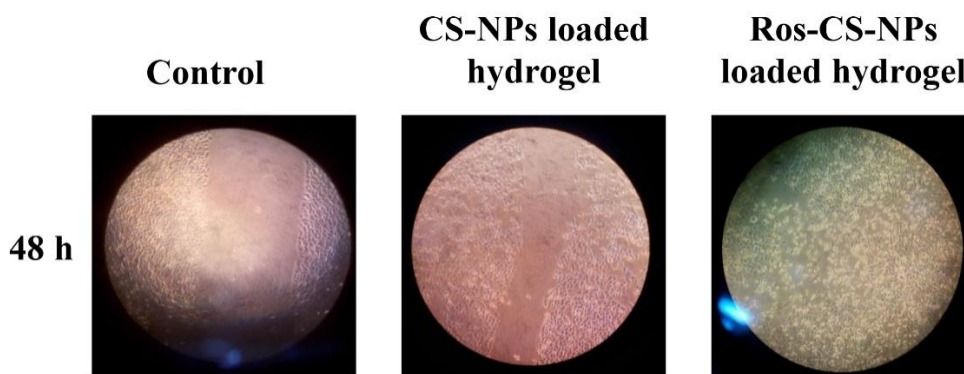


**Figure 2b: Cell migration profile of Ros, CS-NPs loaded hydrogel and Ros-CS-NPs loaded hydrogel.**

### 3.6. Antibacterial activity

Patients with DW commonly experience infections that causes delayed in healing of wounds. The common bacteria out-of-the-way from the infected DWs are *S. aureus* and *E. coli*. The result is shown in fig 3 depicted that the Ros-CS-NPs loaded hydrogel shown a highest inhibitory effect in comparison with that of the CS-NPs loaded hydrogel on *S. aureus*, and *E. coli*. The higher zone of inhibition in the Ros-CS-NPs loaded hydrogel group may be attributed to the synergistic action of Ros & CS.

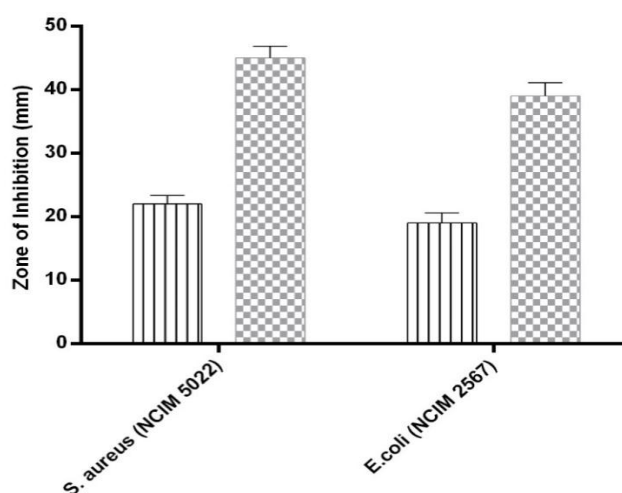


**Figure 3: Anti-bacterial activity of CS-NPs loaded hydrogel and Ros-CS-NPs loaded hydrogel against *S. aureus* and *E. coli*.**

### 3.7. *In vivo* wound healing

The wound area contraction in each group was resolute by using grid technique on day 0, 7, 14 and 21 (fig 4a and 4b). Significant ( $p < 0.05$ ) contraction of wound was observed in Ros-

CS-NPs loaded hydrogel treated group in contrast with that in control and CS-NPs loaded hydrogel treated groups. The mean proportion of wound contraction in Ros-CS-NPs loaded hydrogel treated group was found to be significantly ( $98.46 \pm 4.10\%$  on day 21,  $p < 0.05$ ) faster when compared to control ( $69.77 \pm 4.95\%$  on day 21,  $p < 0.05$ ) and CS-NPs loaded hydrogel ( $79.99 \pm 3.94\%$  on day 21,  $p < 0.05$ ).

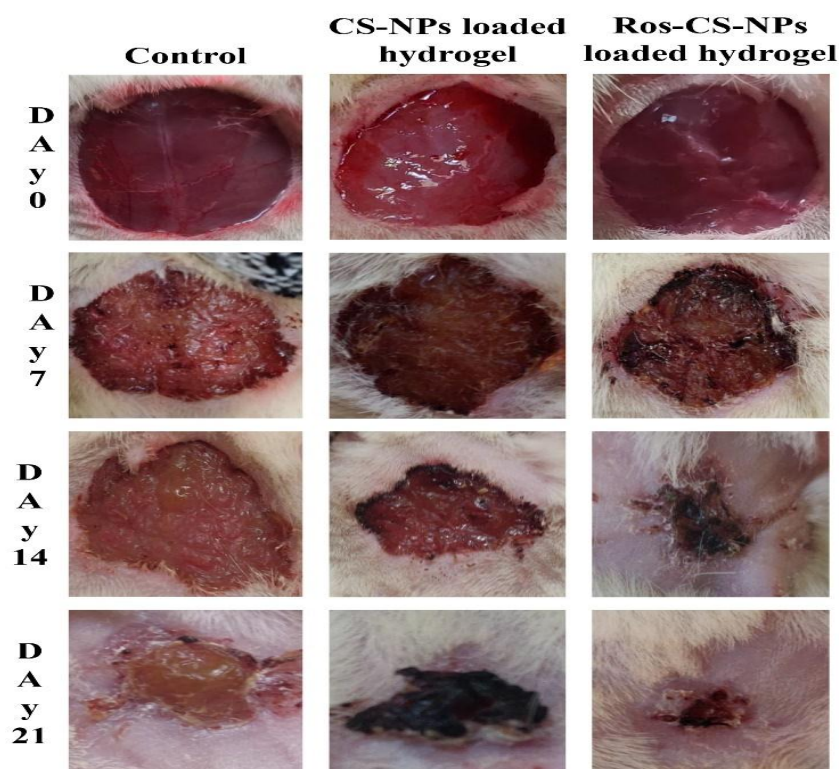


**Figure 4a:** Photographic representation of wound reduction in control, CS-NPs loaded hydrogel and Ros-CS-NPs loaded hydrogel treated group over a period of 21 days.

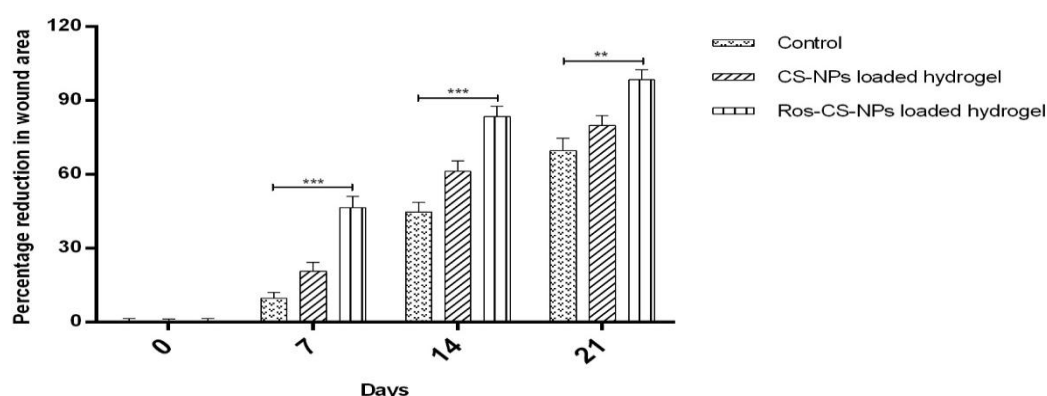


**Figure 4b:** Percentage reduction in mean wound area of wounds in control, CS-NPs loaded hydrogel and Ros-CS-NPs loaded hydrogel treated groups over a period of 21 days.

COL is abundantly available in wound granulation tissue and is synthesized by new fibroblasts. Hydroxyproline content determination indicates the tissue COL amalgamation. The levels hydroxyproline was found to be higher in the Ros-CS-NPs loaded hydrogel treated group as compared with that in the control group. Regardless of the fact that the hydroxyproline content of CS-NPs loaded hydrogel treated group was slightly higher than in Ros-CS-NPs loaded hydrogel treated group, the level was not very significant as shown in fig 5.

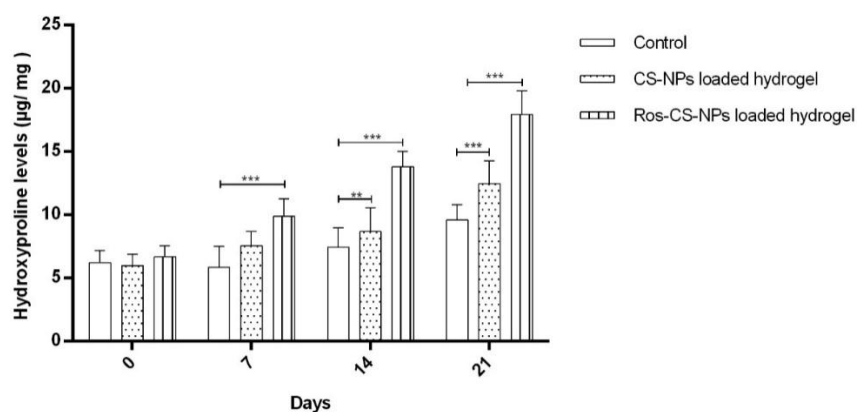


**Figure 5: Hydroxyproline levels in control, CS-NPs loaded hydrogel and Ros-CS-NPs loaded hydrogel treated groups over a period of 21 days.**

### 3.9. Histopathological studies

Histopathological studies exposed that all the wounds were free from oozing on 7th day post injury. Results were depicted in fig. 6. In the CS-NPs loaded hydrogel treated group animals, shown a slighter number of neutrophils and macrophages as compared to control groups. The Ros-CS-NPs loaded hydrogel treated groups exhibited a low number of neutrophils and macrophages in comparison with that of control.

On the 14<sup>th</sup> day post injury, in the control group, neutrophils still prevailed. In the CS-NPs loaded hydrogel treated group, small number of histiocytes and multinucleated massive cells are seen whereas in the Ros-CS-NPs loaded hydrogel treated group plentiful histiocytes, multinucleated giant cells and single lymphocytes were observed.

On the 21<sup>st</sup> day, post injury, the dominant response of inflammation by neutrophils in the control groups was reduced. However, control group showed reappearance of macrophages and histiocytes. The CS-NPs loaded hydrogel group showed moderate number of histiocytes



and lymphocytes. Ros-CS-NPs loaded hydrogel group were found to be rich in histiocytes, multinucleated massive cells and lymphocytes.

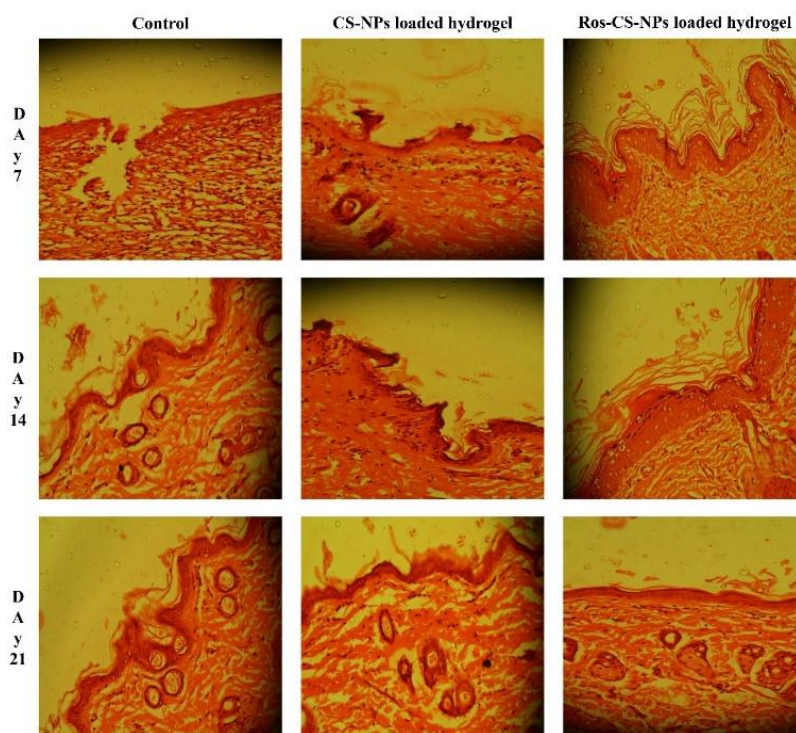


**Figure 6: Histopathological changes in control, CS-NPs loaded hydrogel and Ros-CS-NPs loaded hydrogel treated groups over a period of 21 days.**

### 3.10. ELISA test

MMP-9 content in the Ros-CS-NPs loaded hydrogel and CS-NPs loaded hydrogel treated groups was found to be less in comparison with those of control group. However, MMP-9 content of CS-NPs loaded hydrogel was marginally decreased in contrast with Ros-CS-NPs loaded hydrogel group as shown in fig 7. As described in literature increased levels of MMP-9 are responsible for the breakdown of matrix in wounds. Ros, an anti-inflammatory drug inhibited the MMP-9 levels that may be the reason behind the accumulation of more collagen without breaking resulting in accelerated healing.

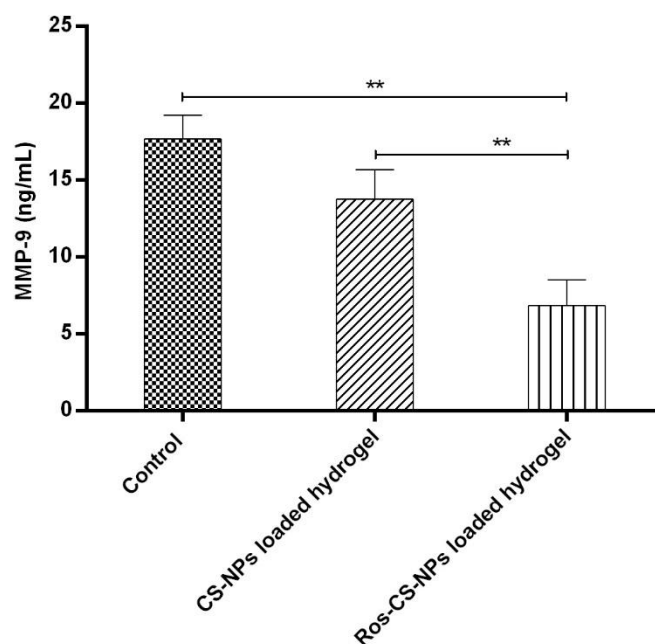


**Figure 7:** MMP-9 levels in control, CS-NPs loaded hydrogel and Ros-CS-NPs loaded hydrogel treated groups over a period of 21 days.

#### 4. CONCLUSION

The formulated novel composite hydrogel fulfilled the prerequisites of an optimum DW dressing in terms of mechanical resilience, controlled release, swelling, biocompatibility, cell bond, with anti-inflammatory properties which are considered to be essential for tissue recovery in DWs. Therefore, current study indicates that the synergistic combination of Ros as an anti-inflammatory agent, CS as a controlled drug carrier and COL as a structural matrix stabilizer which is a likely best approach in treating DWs efficiently. However, further studies are highly needed to understand the molecular mechanism of Ros in treating DWs.

#### Conflict of interest statement

The authors declare that there are no conflicts of interest in this study. The authors alone are responsible for the content and writing of the paper.

#### Funding

This research did not receive any specific grant from funding agencies in the public, commercial, or not-for-profit sectors.



**REFERENCES**

1. Sanapalli BK, Yele V, Kalidhindi RS, Singh SK, Gulati M, Karri VV. Human beta defensins may be a multifactorial modulator in the management of diabetic wound. *Wound Repair and Regeneration*, 2020; 28(3): 416-21.
2. Cho NH KJ, Mbanya JC, Ogurstova K, Guariguata L, Rathmann W. IDF diabetes atlas-eighth. The International Diabetes Federation, 2017.
3. Karri V, Gowthamarajan K, Satish Kumar M, Rajkumar M. Multiple biological actions of curcumin in the management of diabetic foot ulcer complications: a systematic review. *Trop Med Surg*, 2015; 3(179): 2.
4. Yagihashi S, Mizukami H, Sugimoto K. Mechanism of diabetic neuropathy: where are we now and where to go? *Journal of Diabetes Investigation*, 2011; 2(1): 18-32.
5. Natarajan J, Sanapalli BKR, Bano M, Singh SK, Gulati M, Karri VVSR. Nanostructured Lipid Carriers of Pioglitazone Loaded Collagen/Chitosan Composite Scaffold for Diabetic Wound Healing. *Advances in wound care*, 2019; 8(10): 499-513.
6. Allen Jr RJ, Soares MA, Haberman ID, Szpalski C, Schachar J, Lin CD, et al. Combination therapy accelerates diabetic wound closure. *PloS one*, 2014; 9(3): e92667.
7. Karri VNR, Kuppusamy G, Mulukutla S, Sood S, Malayandi R. Understanding the implications of pharmaceutical excipients and additives in the treatment of diabetic foot ulcers. *Journal of Excipients and Food Chemicals*, 2015; 6(1): 7-22.
8. Gupta S. Management of diabetic foot. *MEDICINE*, 2012; 22.
9. Karri VVSR, Kuppusamy G, Talluri SV, Yamjala K, Mannemala SS, Malayandi R. Current and emerging therapies in the management of diabetic foot ulcers. *Current medical research and opinion*, 2016; 32(3): 519-42.
10. Kant V, Gopal A, Pathak NN, Kumar P, Tandan SK, Kumar D. Antioxidant and anti-inflammatory potential of curcumin accelerated the cutaneous wound healing in streptozotocin-induced diabetic rats. *International Immunopharmacology*, 2014; 20(2): 322-30.
11. Mat Saad AZ, Khoo TL, Halim AS. Wound bed preparation for chronic diabetic foot ulcers. *ISRN endocrinology*, 2013; 2013.
12. Falanga V. Wound healing and its impairment in the diabetic foot. *The Lancet*, 2005; 366(9498): 1736-43.
13. Caley MP, Martins VL, O'Toole EA. Metalloproteinases and wound healing. *Advances in wound care*, 2015; 4(4): 225-34.

14. Reiss MJ, Han Y-P, Garcia E, Goldberg M, Yu H, Garner WL. Matrix metalloproteinase-9 delays wound healing in a murine wound model. *Surgery*, 2010; 147(2): 295-302.
15. Gill SE, Parks WC. Metalloproteinases and their inhibitors: regulators of wound healing. *The international journal of biochemistry & cell biology*, 2008; 40(6-7): 1334-47.
16. Bhagavathula N, Nerusu KC, Lal A, Ellis CN, Chittiboyina A, Avery MA, et al. Rosiglitazone inhibits proliferation, motility, and matrix metalloproteinase production in keratinocytes. *Journal of investigative dermatology*, 2004; 122(1): 130-9.
17. Lee C-S, Kwon Y-W, Yang H-M, Kim S-H, Kim T-Y, Hur J, et al. New mechanism of rosiglitazone to reduce neointimal hyperplasia: activation of glycogen synthase kinase-3 $\beta$  followed by inhibition of MMP-9. *Arteriosclerosis, thrombosis, and vascular biology*, 2009; 29(4): 472-9.
18. Marx N, Froehlich J, Siam L, Ittner J, Wierse G, Schmidt A, et al. Antidiabetic PPAR $\gamma$ -activator rosiglitazone reduces MMP-9 serum levels in type 2 diabetic patients with coronary artery disease. *Arteriosclerosis, Thrombosis, and Vascular Biology*, 2003; 23(2): 283-8.
19. Moura LI, Dias AM, Carvalho E, de Sousa HC. Recent advances on the development of wound dressings for diabetic foot ulcer treatment—a review. *Acta biomaterialia*, 2013; 9(7): 7093-114.
20. El-Shabouri M. Positively charged nanoparticles for improving the oral bioavailability of cyclosporin-A. *International journal of pharmaceutics*, 2002; 249(1-2): 101-8.
21. Helary C, Bataille I, Abed A, Illoul C, Anglo A, Louedec L, et al. Concentrated collagen hydrogels as dermal substitutes. *Biomaterials*, 2010; 31(3): 481-90.
22. Calimlioglu B, Karagoz K, Sevimoglu T, Kilic E, Gov E, Arga KY. Archive for the 'CANCER BIOLOGY & Innovations in Cancer Therapy' Category.
23. Balata G, El Nahas HM, Radwan S. Propolis organogel as a novel topical delivery system for treating wounds. *Drug delivery*, 2014; 21(1): 55-61.
24. Sanapalli BKR, Kannan E, Balasubramanian S, Natarajan J, Baruah UK, Karri VVSR. Pluronic lecithin organogel of 5-aminosalicylic acid for wound healing. *Drug development and industrial pharmacy*, 2018; 44(10): 1650-8.
25. Tas C, Özkan Y, Savaser A, Baykara T. In vitro release studies of chlorpheniramine maleate from gels prepared by different cellulose derivatives. *Il Farmaco*, 2003; 58(8): 605-11.
26. Costa P, Lobo JMS. Modeling and comparison of dissolution profiles. *European journal of pharmaceutical sciences*, 2001; 13(2): 123-33.

27. Liang C-C, Park AY, Guan J-L. In vitro scratch assay: a convenient and inexpensive method for analysis of cell migration in vitro. *Nature protocols*, 2007; 2(2): 329.
28. Dash AK, Behera SR, Pattanaik BK, Palo AK. Study of antimicrobial property of some hypoglycemic drugs. *Chronicles of Young Scientists*, 2011; 2(4): 219.
29. Karri VVSR, Kuppusamy G, Talluri SV, Mannemala SS, Kollipara R, Wadhwani AD, et al. Curcumin loaded chitosan nanoparticles impregnated into collagen-alginate scaffolds for diabetic wound healing. *International journal of biological macromolecules*, 2016; 93: 1519-29.
30. Shukla A, Rasik A, Jain G, Shankar R, Kulshrestha D, Dhawan B. In vitro and in vivo wound healing activity of asiaticoside isolated from *Centella asiatica*. *Journal of ethnopharmacology*, 1999; 65(1): 1-11.
31. Nwomeh BC, Liang H-X, Cohen IK, Yager DR. MMP-8 is the predominant collagenase in healing wounds and nonhealing ulcers. *Journal of Surgical Research*, 1999; 81(2): 189-95.
32. Dinarvand R, Moghadam SH, Mohammadyari-Fard L, Atyabi F. Preparation of biodegradable microspheres and matrix devices containing naltrexone. *AAPS Pharm Sci Tech*, 2003; 4(3): 45-54.
33. Zhao Y-N, Xu X, Wen N, Song R, Meng Q, Guan Y, et al. A Drug Carrier for Sustained Zero-Order Release of Peptide Therapeutics. *Scientific Reports*, 2017; 7(1): 5524.